Available online at www.sciencedirect.com
SCIENCE DIRECT
Polymer 46 (2005) 1269–1276
polymer
www.elsevier.com/locate/polymer

Boronic acid-functionalized nanoparticles: synthesis by microemulsion polymerization and application as a re-usable optical nanosensor for carbohydrates

Caroline Cannizzo, Sonia Amigoni-Gerbier, Chantal Larpent*

SIRCOB, UMR-CNRS 8086, Université de Versailles St-Quentin-en-Yvelines, 45 Avenue des Etats-Unis, 78035 Versailles, France

Accepted 30 September 2004
Available online 8 December 2004

Abstract

Translucent boronic acid-carrying nanolatexes are prepared by copolymerisation of vinylbenzyl chloride in microemulsion followed by post functionalisation with 3-aminophenylboronic acid. The diol binding capacity and selectivity of the phenylboronic acid remain unchanged after anchoring to polymer nanoparticles (16 nm diameter, 0.22 mmol/g). The binding of a catechol dye, Alizarin Red S (ARS), to the boronic acid-carrying nanoparticles affords a colored, stable, nanolatex which is used for the selective visual detection of fructose in a competitive assay. The binding of fructose at pH 8.2 is readily evidenced by a color change and monitored by UV/Vis spectroscopy. The nanosensor can be regenerated in acidic medium. The entrapment of the nanolatex in a dialysis cell provides a re-usable support for binding and optical detection.

Keywords: Functionalized nanoparticles; Boronic acid; Optical sensor

1. Introduction

Nowadays, there is a rise in interest in the design of nanoparticulate materials since they were found to impart several advantages owing to their small size and high surface-to-volume ratio [1]. In this context, aqueous suspensions of functionalized polymer nanoparticles, so called 'nanolatexes', hold most promise for the development of new polymer supports with improved reagent activity [2–4]. In life science, polymer nanoparticles have been found to provide valuable supports for the design of carriers, sensors or probes that are suitable for intracellular transport and local measurements [5–9].

The technique of polymerization in microemulsion allows one to produce stable suspensions of ultrafine particles in the nanosize range (i.e. with diameter smaller than 30 nm), nanolatexes, which exhibit very large specific areas (larger than 300 m^2/g) and high surface functionality [2–4,10–15]. The colloidal stability is another outstanding feature of nanolatexes since, under appropriate conditions, microemulsion polymerization leads to very stable and transparent suspensions. Nanolatexes are therefore valuable supports for the design of novel devices for optical sensing since qualitative and quantitative analyses can be readily achieved by classical spectroscopic methods [3–5]. Although the technique of polymerization in microemulsion is now well documented, a limited number of contributions have dealt with the synthesis of functionalized nanoparticles [2–4,12–16]. Consequently, there is a great demand for synthetic approaches that allow the preparation of well-defined nanoparticles that possess chemical or biological functionalities like specific ligands or receptors. An interesting approach for the design of novel devices for sensing, transport or catalysis is to incorporate functional groups to enable the oriented binding of the appropriate guest.

Since boronic acids are known to bind diols through reversible boronate esters formation [17], boronic acid-functionalized nanoparticles may give access to valuable nanosupports for the optical detection, the transport or the

* Corresponding author. Tel.: +33 1 39254413; fax: +33 1 39254452.
E-mail address: larpent@chimie.uvsq.fr (C. Larpent).

0032-3861/$ - see front matter © 2004 Elsevier Ltd. All rights reserved.
doi:10.1016/j.polymer.2004.11.052

separation of carbohydrates. Boronic acid-carrying polymeric materials were developed for carbohydrate recognition [18], specific detection [19,20] or transport [21,22]. Boronic acid-functionalized polymers have also been used for nucleotide isolation [23], drug delivery [24] as well as for affinity chromatography [25]. Some examples of latex functionalized by phenylboronic acid have also been reported [26]. These functional polymeric materials were most often prepared by copolymerization of boronic acid polymerizable derivatives [19,20,23,26] and in some cases by post-functionalization [25,27–29]. Reactions of aminophenylboronic acid APBA with activated esters [25,28] or epoxides [29] have been used to attach phenylboronic residues to polymer backbones.

In this paper we wish to report on the synthesis of boronic acid-functionalized nanoparticles and the study of their diol binding capacity. The binding of a catechol dye, Alizarin Red S (ARS), to the boronic acid-carrying nanoparticles affords an optical colored nanosensor. This nanosensor is used for fructose binding and detection in a competitive assay. Due to its transparency, the supported sensor behaves like previously described soluble molecular sensors [30,31] and the binding of sugar is readily evidenced by a color change. Finally, we show that the entrapment of the nanolatex in a dialysis cell provides a re-usable support for binding and optical detection.

2. Experimental section

Styrene, divinylbenzene (DVB, mixture of isomers, 80%) and vinylbenzylchloride (VBCl, 60/40 mixture of *meta* and *para* isomers) were purchased from Fluka and purified by flash chromatography on silica gel (eluant cyclohexane) before use. Dodecyltrimethylammonium bromide (DTAB, purum, >98%), 3-aminophenyl boronic acid monohydrate (APBA), Alizarin Red S (ARS), phenylboronic acid (PBA) and phosphate buffers were purchased from Fluka and used without further purification. Ultrapure water (milliQ, resistivity >18 MΩ) was used for all experiments.

2.1. Synthesis of the aqueous suspension of boronic acid-carrying nanoparticles: nanolatex NL-B(OH)$_2$

Preparation of reactive nanoparticles NL-CH$_2$X. 304 mg of radical initiator 2,2-dimethoxy-2-phenylacetophenone (DMPA, 0.016 mol/mol of monomers) were added to a mixture of monomers containing 3.2 g of styrene (3.1×10^{-2} mol), 4.1 g of DVB (3.1×10^{-2} mol) and 1.7 g of VBCl (1.1×10^{-2} mol, 15 mol%, 1.22 mmol/g of monomers). A clear transparent microemulsion was prepared by adding under gentle magnetic stirring the mixture of monomers (9 g) to 200 g of a 15 wt% aqueous solution of DTAB. The composition of the starting microemulsion (% wt) is: water 81.3, DTAB 14.4, Styrene 1.5, DVB 2, VBCl 0.8. The freshly prepared microemulsion was transferred in a double-jacketed refrigerated 250 ml schlenk tube and degassed with nitrogen for 30 min. Polymerization was performed at room temperature under white light irradiation using two 50 W lamps for 26 h. A stable, translucent, bluish suspension of reactive particles NL-CH$_2$X was obtained.

Preparation of the boronic acid functionalized nanoparticles NL-B(OH)$_2$. 167 mg of 3-aminophenyl boronic acid monohydrate (1.08×10^{-3} mol, 3.17 equiv. per halogen in NL-CH$_2$X) and 200 μl of NaOH 5N (10^{-3} mol) were added to 10 g of nanolatex NL-CH$_2$X (3.4×10^{-4} mol halogens). The mixture was stirred at room temperature (away from light) for 5 days to yield an ochre suspension. The resulting nanolatex NL-B(OH)$_2$ was purified by dialysis (cellulose membrane, MWCO 12,000) versus a 15% wt aqueous solution of DTAB.

2.2. Characterization of the nanolatexes NL-CH$_2$X and NL-B(OH)$_2$

Quasi-elastic light-scattering analyses were performed at 25 °C with a Brookhaven (BI2030AT) correlator equipped with a 2016 Ar laser (514.5 nm); the measurement angle was 90°. The data were analyzed by the exponential sampling method. The samples were diluted in pure water (0.1 ml of suspension in 9.9 ml of water, polymer concentration 0.04% wt) before analysis. Similar results were obtained at lower polymer concentrations (dilution by 2 and 5). The average diameter was calculated by the cumulant analysis. The illustrative distribution diagrams shown in Fig. 1 were calculated by the non-negatively constrained least squares method (multiple pass).

The polymers were characterized by elemental analyses (obtained from the 'Service central d'analyse', CNRS-Vernaison, France) and IR spectroscopy. The polymer was flocculated by adding 10 ml of methanol to 1 ml of suspension and separated by centrifugation (9900 rpm; 30 min). The resulting paste was washed with 10 ml of

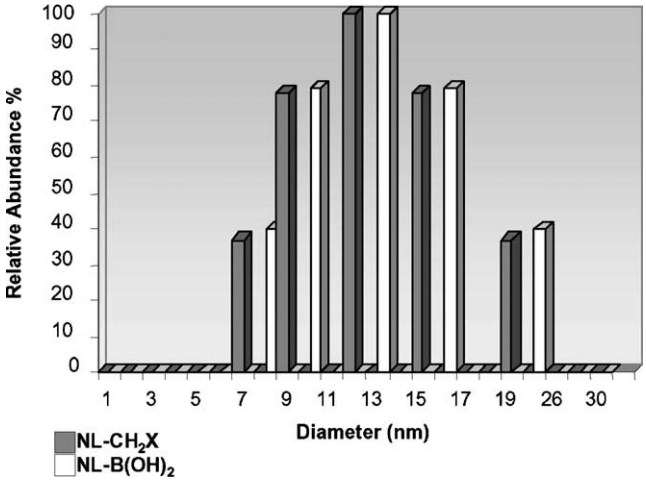

Fig. 1. Size distribution of starting reactive nanoparticles NL-CH$_2$X and boronic acid-functionalized nanoparticles NL-B(OH)$_2$.

water under magnetic stirring at room temperature for 1 h, centrifuged and separated. This washing procedure was repeated at least five times with water. The polymer was dried at 50 °C.

NL-CH_2X. C: 84.04%, H: 7.59%, Cl: 1.32%, Br: 3.86%. Overall halogen content: 0.86 mmol per gram of polymer (0.37 mmol Cl/g; 0.48 mmol Br/g). The halogen concentration (Cl and Br) in NL-CH_2X is 3.4×10^{-2} mol l^{-1}. The nanolatex contains 4% of polymer in weight and 14.4% wt of DTAB. IR (KBr) ν (cm^{-1}): 3017–3083 and 2848–2919 (strong, CH), 1440–1598 (C=C). Size of the nanoparticles: Average diameter 16 ± 2 nm, quadratic polydispersity 0.306. It is worth noticing that QELS analysis of NL-CH_2X has been performed several weeks after its synthesis: this may explain its unusual high polydispersity. For a freshly prepared suspension, using the same procedure, particles with the same average diameter were obtained, with a quadratic polydispersity of 0.079.

NL-B(OH)$_2$. C: 85.18%, H: 7.47%, N: 0.74%, B: 0.25%. The boronic acid content in the polymer, calculated from the boron quantity, is 0.22 mmol/g. The boronic acid concentration in NL-$B(OH)_2$ is 8.8×10^{-3} mol l^{-1}. Polymer content in NL-$B(OH)_2$: 4% wt; 15% wt. DTAB. The excess of nitrogen in the polymer (0.53 mmol/g) may come from the presence of remaining ammonium surfactant in the isolated polymer (the cationic surfactant molecules can be either adsorbed onto the particles surface or associated as counterions with phenylboronate anions). IR (KBr) ν (cm^{-1}): 3396 (strong, O–H), 3017–3083 and 2848–2919 (strong, CH), 1440–1598 (C=C), 1337 (strong, large, B–O). Size of the nanoparticles: Average diameter 15 ± 2 nm, quadratic polydispersity 0.252.

2.3. Binding of the ARS colored dye to the boronic acid functionalized nanoparticles NL-B(OH)$_2$

Absorption spectra were recorded, using 0.2 cm quartz cells, on a Perkin Elmer Spectrophotometer UV/VIS/NIR Lambda 19.

Blank experiments. Association of ARS with phenylboronic acid (PBA) in aqueous buffer. A 5×10^{-3} M solution of ARS was prepared with 10^{-3} M sodium phosphate monobasic buffer (brought to pH 8.2 with HCl 0.1 M). PBA (12.3 mg, 1×10^{-4} mol) was added to 4 ml of the ARS solution to give an ARS-PBA solution containing 5×10^{-3} M ARS and 2.5×10^{-2} M PBA. Both the ARS and ARS + PBA solutions were diluted 10 folds in phosphate buffer (pH 8.2) before analysis. The ARS solution is burgundy (500 nm, $A=0.43$), the ARS–PBA solution is orange (478 nm, $A=0.46$).

Binding of ARS to boronic acid-carrying nanoparticles. Preparation of NL-$B(OH)_2$–ARS. 1.5 ml of NL-$B(OH)_2$ suspension (13.2×10^{-6} mol of boronic acid moieties) were added to 30 ml of the ARS solution (5×10^{-3} M in phosphate buffer, pH 8.2). Upon addition of NL-$B(OH)_2$, an instantaneous change in the color of the ARS solution from burgundy to orange was observed. The suspension remained translucent. The ARS and boronic acid concentrations in the resulting suspension NL-$B(OH)_2$–ARS are, respectively, 4.8×10^{-4} and 4.2×10^{-4} M, molar ratio ARS/boronic acid = 1.1 (from boron content in the polymer). The polymer content in NL-$B(OH)_2$–ARS is 0.19% wt and the concentration of surfactant DTAB is 0.7% wt. NL-$B(OH)_2$–ARS suspension was gently stirred for at least 1 h before UV/Vis measurements (orange, 480 nm, $A=0.44$).

Titration. Aliquots (10 μl) of NL-$B(OH)_2$ were progressively added to 1 ml of ARS (5×10^{-4} M in 10^{-3} M phosphate buffer containing 0.7% DTAB, pH = 8.2). A change in the color of the solution, from burgundy to orange, was observed after addition of 40–60 μl of NL-$B(OH)_2$ i.e. for a concentration of boronic acid moieties between 3.38×10^{-4} and 4.98×10^{-4} M. This corresponds to boronic acid/ARS ratios between 0.7 and 1.05.

Influence of the pH on the binding of ARS, pH stability range of NL-B(OH)$_2$ARS. Absorption spectra of the previously prepared NL-$B(OH)_2$–ARS suspension were recorded at different pH, from pH 1 to 13, by adding small aliquots of NaOH (5, 1 or 0.1 N) or HCl (3, 1 or 0.1 N). Between pH 4 and 10, the nanolatex NL-$B(OH)_2$–ARS remained orange: the absorbance at 478 ± 5 nm was remarkably stable ($A=0.26\pm0.02$). Changes of color and absorption were observed at low and high pH values (maximum absorption wavelengths: 429 nm at pH 2 and 568 nm at pH 12). Free ARS solutions at different pH showed the following absorptions: pH 2: 425 nm; pH 8: 502 nm; pH 12: 555 nm.

2.4. Sugar binding

Sugar binding studies were performed by adding the desired amount of sugar (D-fructose or/and D-glucose, 1.8–900 mg, concentrations range: 5×10^{-3}–2.5 M) as a solid to 2 ml of NL-$B(OH)_2$–ARS suspension (previously prepared, pH 8.2). The samples were stirred for 2 h before spectrophotometric measurements.

2.5. Entrapment and re-use of the nanosensor NL-B(OH)$_2$–ARS

NL-$B(OH)_2$–ARS suspension (2 ml) were dialyzed overnight towards a phosphate buffer (10^{-3} M, pH 8.2) containing 0.7% wt DTAB. The absorption spectrum was not modified after dialysis (orange, 484 nm, $A=0.42$).

2.5.1. Fructose detection (step 1)

NL-$B(OH)_2$–ARS was transferred into two 1 ml dialysis cells (cellulose membrane, MWCO 12,000): a reference cell and a measurement cell. The measurement cell (M) was immersed in phosphate buffer (10^{-3} M, pH 8.2) containing 0.7% wt DTAB and fructose 0.25 M. The reference cell (R) was immersed in phosphate buffer (10^{-3} M, pH 8.2)

containing 0.7% wt DTAB without fructose. UV/Vis spectra were recorded after two hours. M: burgundy (498 nm, $A=0.38$). R: orange (485 nm, $A=0.39$), $\Delta\lambda_{M/R}=13$ nm.

2.5.2. Recovery of the NL-B(OH)$_2$–ARS nanosensor (step 2)

Decomplexation of fructose was achieved at pH 4. Both measurement and reference cells were immersed in a pH 4 aqueous solution containing 0.7% wt DTAB and dialyzed overnight. M: 487 nm, $A=0.38$. R: 487 nm, $A=0.38$, $\Delta\lambda_{M/R}=0$ nm. Before being re-used for sugar detection, both cells were dialyzed versus a phosphate buffer solution (10^{-3} M, pH $=8.2$, containing 0.7% wt DTAB) during one night.

2.5.3. Re-use of NL-B(OH)$_2$–ARS for fructose detection (step 3)

A second detection experiment was performed as described above (step 1). M: 502 nm, $A=0.38$. R: 489 nm, $A=0.34$, $\Delta\lambda_{M/R}=13$ nm.

3. Results and discussion

3.1. Synthesis and characterization of the boronic acid nanoparticles

Although post-functionalisation of classical latexes is well documented, there are only few examples of chemical modification of nanoparticles prepared by microemulsion polymerization [2,14–16]. We have previously shown that functionalized nanoparticles can be efficiently prepared by linking amines to nanoparticles carrying chloromethyl or activated ester reactive groups [2,14,15]. In the present work, we choose to introduce the boronic acid functionalities by reacting readily accessible benzylhalide-functionalized polymer nanoparticles with 3-aminophenylboronic acid (APBA). The boronic acid-functionalized nanolatex NL-B(OH)$_2$ is prepared in two steps using the procedure described in Scheme 1.

The starting aqueous suspension of nanoparticles, nanolatex NL-CH$_2$X, bearing reactive benzylhalide surface-end groups is prepared by polymerization in ternary oil-in-water microemulsion stabilized with a cationic surfactant (dodecyltrimethylammonium bromide: DTAB). Copolymerization of vinylbenzylchloride (15 mol%, 1.22 mmol/g of monomers) with styrene and divinylbenzene as a cross-linking agent is performed in the presence of a radical photo-initiator DMPA (2,2-dimethoxy-2-phenylacetophenone) solubilized within the monomers oil phase [3,4,14,15]. Polymerization readily takes place at room temperature under white light irradiation and leads to a stable, translucent, slightly bluish, colloidal aqueous suspension of nanoparticles NL-CH$_2$X (Fig. 2, S1). The average diameter of the nanoparticles, determined by quasi-elastic light scattering, is 16 nm with an acceptable size distribution (Fig. 1); the polymer load in nanolatex NL-CH$_2$X is 4% wt in agreement with a complete polymerization of the monomers. The overall content of reactive benzylhalide residues in the nanoparticles, deduced from elemental analyses of the isolated and purified polymer, is about 0.86 mmol/g. The deficit of chlorine (0.38 mmol/g) as well as the presence of bromine (0.48 mmol/g) in the polymer clearly indicate that both exchange of chlorine for bromine and partial hydrolysis of the benzyl chloride groups occur during the polymerization process. About 40% of the chlorine atoms have been substituted by bromine and 30% have been hydrolyzed. The large excess of bromide anions introduced as surfactant counterions in the starting microemulsion accounts for the observed Cl per Br substitution (the molar ratio DTAB/VBCl is about 10) [15]. Similar nucleophilic substitutions have been observed in micellar solutions of ammonium bromide surfactants [32]. If one considers the following post-functionalization step, this substitution is profitable because it transforms benzylchloride groups into more reactive benzylbromide residues. On the other hand, hydrolysis of the benzylhalide moieties produces non-reactive benzylalcohol residues, hence it is highly preferable to perform the following functionalization step on freshly prepared nanolatexes. The overall content of benzylhalide residues is large enough to ensure the post-grafting of acceptable amounts of functional groups [15]. Further experiments have shown that about 40–45% of the benzylhalide residues are accessible for surface reactions (i.e. located near the surface) and that the halogens embedded within the particle core (about 55–60%) do not participate and remain after post-functionalization.

The covalent linkage of boronic acid residues to the nanoparticles is readily achieved by reacting 3-aminophenylboronic acid APBA with the as-prepared nanolatex NL-CH$_2$X at room temperature. The maximum functionalization yield is obtained when the reaction is performed with an excess of APBA (2 or 3 equiv. per benzylhalide), in the presence of one equiv. of NaOH per APBA for 3 days. The presence of stoichiometric amount of base avoids the acidification of the medium and ensures that most of the APBA molecules are negatively charged (the pK_a values for boronic acid ionization and for amine protonation in APBA are 8.37 and 4.52, respectively) [33]. Ionic attractions between cationic surfactant molecules adsorbed onto the particles and aminophenylboronate anions may favor the surface reaction, as previously observed with other nucleophiles [2,14]. After removal of the excess of reagent by dialysis, an ochre translucent boronic acid-functionalized nanolatex NL-B(OH)$_2$ is obtained (Fig. 2, S2).

The amount of boronic acid residues in the polymer, deduced from boron elemental analysis of the separated and cleaned polymer, is 0.22 mmol/g. The overall concentration of phenylboronic acid in the aqueous nanolatex NL-B(OH)$_2$ is 8.8×10^{-3} mol l^{-1}. The post-functionalization yield is about 60% with respect to the accessible benzylhalide surface end groups in NL-CH$_2$X. Competitive hydrolysis of

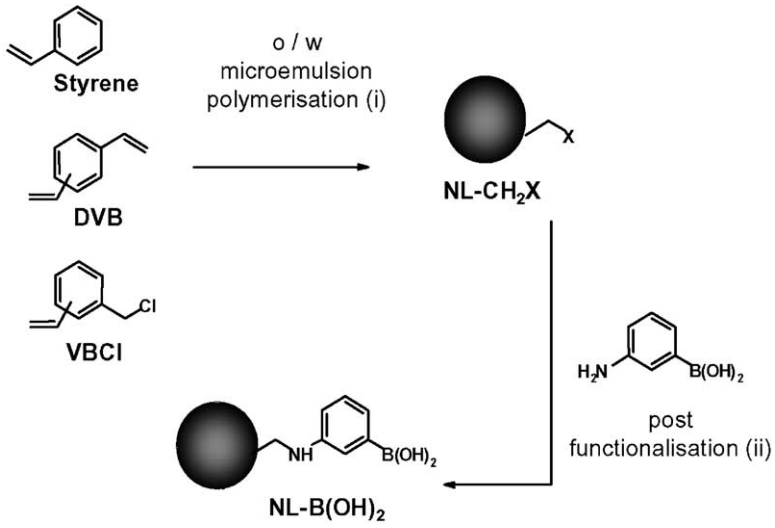

Scheme 1. Preparation of the boronic acid-functionalized nanoparticles: (i) initiator: 2,2-dimethoxy-2-phenylacetophenone (DMPA), surfactant: dodecyl trimethylammonium bromide (DTAB), room temperature, 26 h, (ii) 3.2 equiv., room temperature, 5 days.

the benzylhalide residues may account for the limited substitution yield.

As shown in Fig. 1, the particles sizes and distribution remain unchanged upon functionalization. The simple and straightforward procedure depicted here thus gives access to nanoparticles with an average diameter of 16 nm that contain about 280–320 boronic acid residues per particle. Moreover, the boronic acid-functionalized nanolatex NL-$B(OH)_2$ is stable for several months and the amount of surfactant can be reduced to less than 1% in weight by dialysis without any observable aggregation of the particles.

3.2. Binding of the ARS dye to boronic acid-carrying nanoparticles: preparation of the optical nanosensor NL-$B(OH)_2$–ARS

Phenylboronic acid is known to bind the colored dye Alizarin Red S (ARS) with high association constants over a wide range of pH (Table 1) [30,34]. ARS displays a dramatic change in color and fluorescence intensity in response to the binding of boronic acid. ARS has been successfully used as an optical reporter for the detection of sugars in buffered aqueous solutions in competitive assays [30,31]. The binding of ARS to nanolatex NL-$B(OH)_2$ may thus give access to a supported optical nanosensor through reversible boronate ester formation (Scheme 2).

Upon addition of nanolatex NL-$B(OH)_2$ the color of an aqueous solution of ARS (5×10^{-4} M, pH 8.2) changes from burgundy to orange thus indicating the binding of ARS to nanoparticles (Scheme 2; Fig. 2, S3 and S4). Taking profit of the transparency of the nanolatexes, the formation of the ARS–boronic acid complex can also be monitored by UV/Vis spectroscopy (free ARS $\lambda_{max}=502$ nm; ARS boronate ester $\lambda_{max}=480$ nm, Fig. 3). Remarkably, the color change occurs instantaneously under conditions close to stoichiometry thus demonstrating the accessibility of the boronic acid receptors grafted to nanoparticles. A similar solution-like behavior has already been observed for metal-complexing nanoparticles [3,4]. As can be seen in Fig. 2, the binding of ARS does not alter the colloidal stability: the aqueous suspension of ARS boronate-carrying nanoparticles NL-$B(OH)_2$–ARS is stable and translucent. Nanolatex

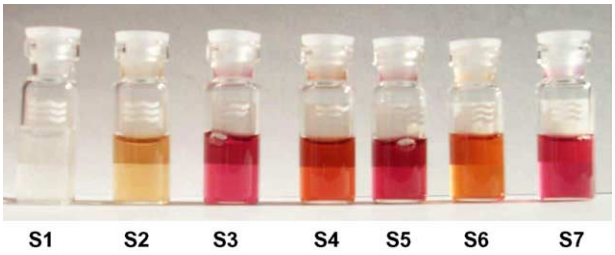

Fig. 2. Photographs of the different samples. S1: NL-CH_2X. S2: NL-$B(OH)_2$ (4.2×10^{-4} M boronic acid moieties) (Fig. 3(a)). S3: ARS (5×10^{-4} M; phosphate buffer 10^{-3} M, pH = 8.2). $\lambda_{max}=502$ nm, $A=0.42$ (Fig. 3(b)). S4: NL-$B(OH)_2$–ARS (4.8×10^{-4} M ARS, 4.2×10^{-4} M boronic acid moieties; phosphate buffer 10^{-3} M, pH = 8.2). $\lambda_{max}=482$ nm, $A=0.44$ (Fig. 3(c)). S5: NL-$B(OH)_2$–ARS + fructose (0.25 M). $\lambda_{max}=492$ nm, $A=0.38$ (Fig. 3(d)). S6: NL-$B(OH)_2$–ARS + glucose (2.5 M). $\lambda_{max}=486$ nm, $A=0.44$. S7: NL-$B(OH)_2$–ARS + fructose (0.25 M) and glucose (2.5 M). $\lambda_{max}=492$ nm, $A=0.40$.

Table 1
Association constants (K_{eq}, M^{-1}) of the ester formed with phenylboronic acid, at various pH in 0.1 M phosphate buffer [34]

pH	ARS	Fructose	Glucose
4.6	190		
5.8	990	4.6	
6.5	1200	29	0.84
7.0	1500	92	2.0
7.4	1300	160	4.6
8.0	670	310	7.2
8.5	450	560	11

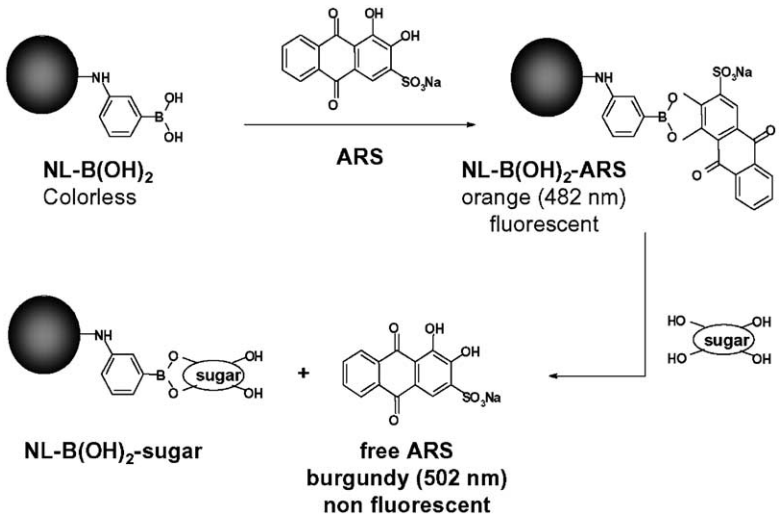

Scheme 2. Competitive assay: binding of the dye (ARS) and dissociation in the presence of a carbohydrate.

NL-B(OH)$_2$–ARS contains about 1.9 g of polymer nanoparticles per liter and 0.7% wt of surfactant DTAB.

Since the pH affects the affinity of boronic acids towards diols, we have examined the pH profile of NL-B(OH)$_2$–ARS in order to determine the stability range. The absorbance of ARS boronate in NL-B(OH)$_2$–ARS remains constant from pH 4 to pH 10. At low pH, the boronic acid–ARS complex dissociates. At high pH, the formation of an ionized tetrahedral derivative has been proposed [34].

3.3. Selective detection of fructose

Owing to its chemical and colloidal stability, NL-B(OH)$_2$–ARS may be used as a supported nanosensor over a wide range of pH thus offering the opportunity to bind and detect various carbohydrates and hydroxylated solutes in competitive assays. A competitive assay requires that the receptor (here the supported boronic acid) and the reporter (here the ARS dye) associate under the measurement conditions. The receptor–reporter complex (here the boronic acid–ARS complex) is then selectively dissociated in the presence of the appropriate guest [30,31]. Phenylboronic acid has a high affinity for D-fructose in basic medium. The values of the association constants reported in Table 1 indicate that fructose competes with ARS at pH >8.

As shown in Fig. 2, the binding of fructose to boronic acid-functionalized nanoparticles is easily evidenced by the color change of NL-B(OH)$_2$–ARS suspension at pH 8.2 from orange to burgundy (release of free ARS): the nanosensor allows the visual detection of fructose (visual detection limit: 0.2 M). The binding of fructose can also be monitored by UV/Vis absorption ($\lambda_{max}=492$ nm, $\Delta\lambda=10$ nm, Fig. 3). Titrations with increasing concentrations of fructose clearly evidence the displacement of ARS by fructose: The calibration plot given in Fig. 4 shows that the decrease of absorbance of the ARS–boronate ester at

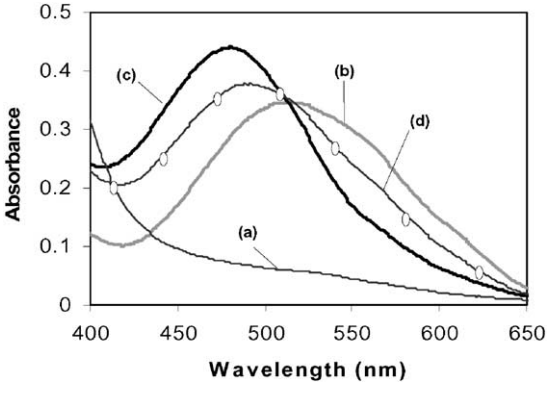

Fig. 3. Absorption spectra, phosphate buffer (10^{-3} M), pH $=8.2$. (a) NL-B(OH)$_2$ (4.2×10^{-4} M boronic acid moieties). (b) ARS (4.8×10^{-4} M, in the presence of 0.7% wt DTAB). (c) NL-B(OH)$_2$–ARS (4.8×10^{-4} M ARS, 4.2×10^{-4} M boronic acid moieties). (d) NL-B(OH)$_2$–ARS $+0.25$ M fructose.

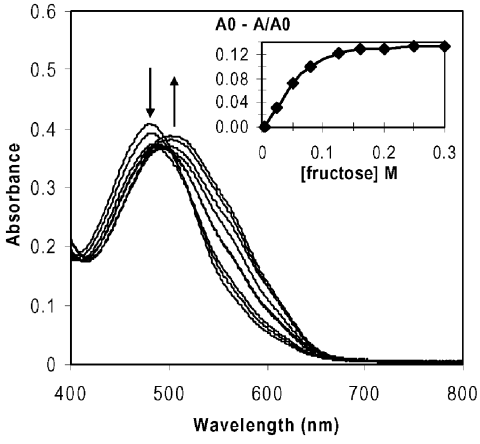

Fig. 4. Absorption spectral changes of NL-B(OH)$_2$–ARS with increasing concentration of D-fructose. Phosphate buffer (10^{-3} M, pH $=8.2$), Concentrations of fructose from 5×10^{-3} to 2.5 M. Inset: calibration plot, relative variation of absorbance at 480 nm.

480 nm allows the quantification of fructose concentrations in the 0.02–0.1 M range.

On the other hand, in good agreement with the values of the association constants (Table 1), D-glucose does not perturb the ARS-supported boronic acid equilibrium: the color of NL-$B(OH)_2$–ARS is not altered by the addition of glucose even at high concentration: 2.5 M (Fig. 2, S6). As the binding constant of D-glucose towards a phenylboronic acid is much lower than the binding constant of D-fructose around pH 8, the complexation should be clearly in favor of fructose (Table 1). We indeed observe a selective recognition of fructose over glucose by our nanosensor NL-$B(OH)_2$–ARS: as shown in Fig. 2, NL-$B(OH)_2$–ARS color changes from orange to burgundy in the presence of fructose and a 10-fold excess of glucose ($\Delta\lambda = 10$ nm). These results clearly indicate that the selectivity of phenylboronic acid remains unchanged after anchoring to polymer nanoparticles.

The selective binding of a given carbohydrate in the presence of other carbohydrates is always an interesting challenge for the development of specific sensors and separation processes [22]. Our boronic acid-functionalized nanoparticles may therefore find valuable applications for the selective separation of fructose from mixtures.

3.4. Development of a stable re-usable optical nanosensor entrapped within a dialysis cell

The binding constant of fructose with phenylboronic acid is highly sensitive to the pH and hence fructose boronate esters readily dissociate at slightly acidic pH (Table 1) [34]. On the other hand, the boronic acid–ARS complex is much less sensitive to a decrease of pH and, as previously mentioned, the doped nanolatex NL-$B(OH)_2$–ARS remains stable down to pH 4. Accordingly, the nanosensor NL-$B(OH)_2$–ARS is readily regenerated by dialysis in a pH 4 buffer after fructose detection. NL-$B(OH)_2$–ARS recovers its original color. A slight decrease of absorbance, which corresponds to the release of less than 10% of ARS, is observed.

Moreover, the aqueous nanolatex NL-$B(OH)_2$–ARS, when entrapped in a dialysis cell with a membrane cut-off of 12,000, remains sensitive to the presence of fructose in the outer solution. The characteristic change of color from orange ($\lambda_{max} = 484$ nm) to burgundy ($\lambda_{max} = 498$ nm) is observed when the cell is immersed in a 0.25 M solution of fructose at pH 8.2. The readily separated cell-entrapped aqueous nanosensor NL-$B(OH)_2$–ARS is then regenerated by dialysis towards pH 4 buffer and can be re-used for further detections of fructose.

The entrapment in a dialysis cell thus provides a stable re-usable optical supported nanosensor suitable for fructose detection in dilute medium. The binding of fructose to the cell-entrapped nanoparticles may provide efficient systems for its selective separation from carbohydrates mixtures.

4. Conclusion

Microemulsion copolymerization followed by post-functionalization with APBA is a straightforward, simple, synthetic pathway to boronic acid-carrying nanoparticles. The stable and translucent functionalized nanolatexes behave like soluble macromolecular supports with comparable accessibility of the boronic acid receptors. Phenylboronic acid grafted on the nanoparticles retain its binding capacity and selectivity for diols so that the functionalized nanolatexes can be turned to colored optical sensors by association with a catechol dye and used in competitive assays. The entrapment of the nanolatex in a dialysis cell provides a re-usable support for binding and optical detection as well as selective separation of fructose.

The procedure, depicted here with ARS, is hoped to be quite general for the obtention of a variety of diol-responsive colored nanolatexes through reversible binding of different dihydroxylated dyes.

Owing to their reversible binding capacity and their size, boronic acid-functionalized nanoparticles hold most promise in biology and in medicine for example for nucleotides isolation and intracellular transport as well as drug delivery.

Acknowledgements

The French Ministry of Research, Program ACI Nanostructures-2000, is greatfully acknowledged for fundings and studentship to CC. We thank Sylvain Desert (CEA-Saclay) for QELS analyses and Barbara Hennequin (graduate student) for technical help.

References

[1] Niemeyer CM. Angew Chem Int Ed 2001;40(22):4128–58.
[2] Larpent C. In: Elaissari A, editor. Colloidal polymers. Surfactant science series, vol. 115. New York: Marcel Dekker; 2003. p. 145–87 (chapter 7).
[3] Amigoni-Gerbier S, Larpent C. Macromolecules 1999;32(26): 9071–3.
[4] Amigoni-Gerbier S, Desert S, Gulik-Kryswicki T, Larpent C. Macromolecules 2002;35(5):1644–50.
[5] Park EJ, Brasuel M, Behrend C, Philbert MA, Kopelman R. Anal Chem 2003;75(15):3784–91.
[6] Davda J, Labhasetwar V. Int J Pharm 2002;233(1–2):51–9.
[7] Sumner JP, Aylott JW, Monson E, Kopelman R. Analyst 2002;127(1): 11–16.
[8] Kürner JM, Wolfbeis OS, Klimant I. Anal Chem 2002;74(9):2151–6.
[9] Lu J, Rosenzweig Z, Fresenius J. Anal Chem 2000;366(6–7):569–75.
[10] Hentze HP, Kaler EW. Curr Opin Colloid Interf Sci 2003;8(2): 164–78.
[11] (a) Candau F. In: Kumar P, Mittal KL, editors. Handbook of microemulsion science and technology. New York: Marcel Dekker; 1999. p. 679–712, chapter 22.
(b) Candau F. In: Paleos CM, editor. Polymerization in organized media. Philadelphia: Gordon & Breach; 1992. p. 215–82 (chapter 4).

[12] Antonietti M, Basten R, Lohmann S. Macromol Chem Phys 1995; 196(2):441–66.
[13] Larpent C, Bernard E, Richard J, Vaslin S. Macromolecules 1997; 30(3):354–62.
[14] Larpent C, Bernard E, Richard J, Vaslin S. React Funct Polym 1997; 33(1):49–59.
[15] Larpent C, Amigoni-Gerbier S, de Sousa Delgado AP. C R Chimie 2003;6(11-12):1275–83.
[16] Li P, Xu J, Wu C. J Polym Sci A: Polym Chem 1998;36(12):2103–9.
[17] Striegler S. Curr Org Chem 2003;7(1):82–102.
[18] Kitano H, Kuwayama N, Ohno K. Langmuir 1998;14(1):165–70.
[19] Gao S, Wang W, Wang B. Bioorg Chem 2001;29(5):308–20.
[20] Appleton B, Gibson TD. Sens Actuators B 2000;65(1–3):302–4.
[21] Mulla HR, Agard NJ, Basu A. Bioorg Med Chem Lett 2004;14(1): 25–7.
[22] Di Luccio M, Smith BD, Kida T, Borges CP, Alves TLM. J Membr Sci 2000;174(2):217–24.
[23] (a) Senel S, Camli ST, Tuncel M, Tuncel A. J Chromatogr B 2002; 769(2):283–95.
(b) Elmas B, Onur MA, Senel S, Tuncel A. Colloids Surf A 2004; 232(2–3):253–9.
[24] Shiino D, Murata Y, Kubo A, Kim YJ, Kataoka K, Koyama Y, Kikuchi A, Yokoyama M, Sakurai Y, Okano T. J Controlled Rel 1995; 37(3):269–76.
[25] Koyama T, Terauchi KI. J Chromatogr B 1996;679(1–2):31–40.
[26] Hazot P, Delair T, Elaissarï A, Chapel JP, Pichot C. Colloid Polym Sci 2002;280(7):637–46.
[27] Sebastian RM, Magro G, Caminade AM, Majoral JP. Tetrahedron 2000;56(34):6269–77.
[28] Uguzdogan E, Kayi H, Denkbas EB, Patir S, Tuncel A. Polym Int 2003;52(5):649–57.
[29] Camli ST, Senel S, Tuncel A. Colloids Surf A 2002;207(1–3):127–37.
[30] Arimori S, Ward CJ, James TD. Tetrahedron Lett 2002;43(2):303–5.
[31] Springsteen G, Wang B. Chem Commun 2001;(17):1608–9.
[32] Martin CA, McCrann PM, Angelos GH, Jaeger DA. Tetrahedron Lett 1982;23(45):4651–4.
[33] Asher SA, Alexeev VL, Goponenko AV, Sharma AC, Lednev IK, Wilcox CW, Finegold DN. JACS 2003;125(11):3322–9.
[34] Springsteen G, Wang B. Tetrahedron 2002;58(26):5291–300.